# Contrasting photosynthesis and photoinhibition in tetraploid and its autodiploid honeysuckle (*Lonicera japonica* Thunb.) under salt stress

*Kun Yan[1,2]\*, Congwen Wu[1,2,3], Lihua Zhang[1,2] and Xiaobing Chen[1,2]\**

[1] *Key Laboratory of Coastal Environmental Processes and Ecological Remediation, Yantai Institute of Coastal Zone Research, Chinese Academy of Sciences, Yantai, China,* [2] *Shandong Provincial Key Laboratory of Coastal Environmental Processes, Yantai Institute of Coastal Zone Research, Chinese Academy of Sciences, Yantai, China,* [3] *Academy of Life Sciences, Yantai University, Yantai, China*

Honeysuckle (*Lonicera japonica* Thunb.) is a popular landscape plant. This study was to explore leaf photosynthetic characterization with emphasis on the coordination between photosystem II (PSII) and photosystem I (PSI) in tetraploid and its autodiploid honeysuckle (TH and DH) upon salt stress (300 mM NaCl). Leaf photosynthetic rate and carboxylation efficiency in DH and TH were significantly decreased under salt stress, and the decrease was greater in DH. PSII photoinhibition was induced in DH under salt stress, as the maximum quantum yield of PSII (Fv/Fm) was significantly decreased. PSII photoinhibition declined electron flow to PSI, but did not prevent PSI photoinhibition, as the maximal photochemical capacity of PSI ($\triangle MR/MR_0$) was significantly decreased by salt stress. According to the significant decrease in PSI oxidation amplitude in the first 1 s red illumination, PSI photoinhibition was more severe than PSII photoinhibition. As a result, PSII and PSI coordination was destroyed. Comparatively, salt-induced photoinhibition did not occur in TH, as no significant change was observed in Fv/Fm and $\triangle MR/MR_0$. Consequently, PSII and PSI coordination was not significantly affected by salt stress. In conclusion, TH maintained normal coordination between PSII and PSI by preventing photoinhibition and exhibited higher leaf photosynthetic activity than DH under salt stress. Compared with DH, lower leaf ionic toxicity due to greater root $Na^+$ extrusion and restriction of $Na^+$ transport to leaf might be responsible for maintaining higher leaf photosynthetic capacity in TH under salt stress.

Keywords: honeysuckle, $Na^+$, photosystem, photosynthetic electron transport, polyploidy

## Introduction

Salinity is one of the main abiotic stresses which reduce plant growth and development. Salt stress can damage biological macromolecules and interfere with metabolisms in plant cells by inducing osmotic stress and ionic toxicity (Munns and Tester, 2008). Photosynthesis closely correlates with

**Abbreviations:** CE, carboxylation efficiency; Ci, intercellular $CO_2$ concentration; DH, diploid honeysuckle; ETo/ABS, quantum yield for electron transport; Fv/Fm, the maximal quantum yield of PSII; $g_s$, stomatal conductance; MDA, malondialdehyde; $\triangle MR/MR_0$, the maximal photochemical capacity of PSI; NMT, non-invasive micro-test technique; NPQ, non-photochemical quenching; OEC, oxygen-evolving complex; Pn, Photosynthetic rate; PSI, photosystem I; PSII, photosystem II; ΦPSII, actual photochemical efficiency of PSII; ROS, reactive oxygen species; Rubisco, ribulose-1,5-bisphosphate carboxylase/oxygenase; TH, tetraploid honeysuckle; $W_k$, variable fluorescence intensity at K step.

plant growth and is sensitive to salt stress, and photosynthetic capacity is an important criterion for diagnosing plant adaptability to salinity (Kalaji and Pietkiewicz, 1993; Kalaji et al., 2011).

Up to now, the effects of salt stress on plant photosynthesis have been extensively studied. The decreased $CO_2$ availability due to the diffusion limitation of stomata is considered as the initial negative effect of salt stress on photosynthesis (Loreto et al., 2003; Chaves et al., 2009). Rubisco is a crucial enzyme in $CO_2$ fixation process. Salt stress can suppress Rubisco activity by reducing Rubisco content and activation, and lead to the decline of $CO_2$ fixation (Feng et al., 2007; Lu et al., 2009). The inhibition on $CO_2$ assimilation will increase accumulation of reducing equivalents in the form of NADPH, underlie over-reduction of photosynthetic electron transport chain and elevate excitation pressure in chloroplast. If the excess excitation energy cannot be dissipated, ROS production will be increased and then bring about photoinhibition (Muller et al., 2001; Takahashi and Murata, 2008). NPQ plays a major role in photoprotection, as it can dissipate the excess excitation energy from light as heat and lower the creation of ROS (Bilger and Bjorkman, 1990; Carbonera et al., 2012; Brestic et al., 2014). PSII photoinhibition is a result of the imbalance between PSII photodamage and the repair of such damage (Murata et al., 2007). PSII photodamage is initiated by the direct effect of light on the OEC, and ROS inhibit the repair of photodamaged PSII mainly by suppressing the synthesis of D1 protein. In the existing studies, it is not consistent whether salt stress can induce PSII photoinhibition, possibly due to the different plant materials and salt treatment protocols (Chen et al., 2004; Netondo et al., 2004; Kalaji et al., 2011; Hussain et al., 2012; Chen et al., 2013). In contrast, few studies pay attention to the salt effects on PSI capacity in plants (Stepien and Johnson, 2009). PSI photoinhibition is induced by ROS produced at the acceptor side of PSI through Mehler reaction *in vivo* (Sonoike, 2011). The electron flow from PSII is essential for PSI photoinhibition, and the addition of 3-(3,4-dichlorophenyl)-1,1-dimethylurea, an inhibitor of PSII primary electron acceptor oxidation, can suppress PSI photoinhibition and help PSI recovery after photoinhibition (Sonoike, 1996; Zhang et al., 2011). PSI photoinhibition is more dangerous than PSII photoinhibition because of the difficult recovery process of PSI (Kudoh and Sonoike, 2002; Zhang and Scheller, 2004). Therefore, rapid PSII photoinhibition under high temperature or high light stress protects PSI from photoinhibition by restricting the electron flow to PSI (Herrmann et al., 1997; Yan et al., 2013a,b; Zivcak et al., 2014). PSI photoinhibition usually arises under chilling stress with low light because of the limited restriction on electron flow to PSI, and in particular, rapid recovery of PSII after chilling stress is detrimental to the recovery of PSI (Zhang et al., 2011). Thus, PSII and PSI coordination plays an important role in protecting PSI or even the whole photosynthetic apparatus. However, it is still largely unknown about the interaction between PSII and PSI in plants under salt stress.

Polyploidy indicates the doubling of chromosomes of a single species or the hybrids between two species, and polyploidy usually can enhance plant tolerance to abiotic stresses. In contrast to the diploid, polyploid black locust, turnip and *Arabidopsis*

exhibited stronger salt tolerance with less decrease in biomass and lower accumulation of leaf $Na^+$ under salt stress (Meng et al., 2011; Chao et al., 2013; Wang et al., 2013). On the contrary, Mouhaya et al. (2010) reported that tetraploid citrus accumulated more $Na^+$ in the leaf and showed greater decrease in PSII capacity than diploid citrus. Therefore, it is not confirmed whether polyploidy can enhance plant salt tolerance. Photosynthetic characterization, especially for PSII and PSI interaction, has not been deeply explored in polyploid plant under salt stress.

Honeysuckle, a twining semi-evergreen vine, is a popular landscape plant with high environmental adaptability and distributed widely in temperate and tropical regions. TH has less whole plant leaf area, higher leaf mass per unit area, thicker epidermis, and palisade tissue as well as denser pubescence compared with its diploid progenitor, and the stronger drought tolerance in TH originates from these morphological characterizations (Li et al., 2009). In this study, we intended to reveal photosynthetic characterization with emphasis on PSII and PSI coordination in tetraploid and its autodiploid honeysuckle and discriminate their salt tolerance. Our study can deepen the knowledge of salt tolerance mechanism in polyploid plants and may provide a reference for cultivar selection in saline land greening.

## Materials and Methods

### Plant Material and Treatment

Stem cuttings from two cultivars of honeysuckle, tetraploid (Jiufengyihao, 36 chromosomes) and its diploid progenitor (Damaohua, 18 chromosomes) were bought from jiujianpeng agricultural technology limited company (Pingyi, Shandong, China). The tetraploid cultivar was bred by treating the stem tips of a diploid cultivar with colchicines (Li et al., 2009). The cuttings were planted in a nursery in November, 2013, and then transplanted to the plastic pots filled with quartz sand in April, 2014. The plants were watered with Hoagland solution (pH 5.7) and placed in climatic chambers (Huier, China). The photon flux density was approximately 200 $\mu mol\ m^{-2}\ s^{-1}$ (12 h per day from 07:00 to 19:00) in the chambers. Day/night temperature and humidity were controlled at 25/18°C and 65% in the chambers. After 60 days, healthy and uniform plants were selected for salt treatments. NaCl was added to nutrient solution incrementally by 50 mM step every day to provide final concentration of 300 mM. Nutrient solution without adding NaCl was used to cultivate the control plants. The expanded leaves from the middle of a shoot were sampled for measuring photosynthetic parameters and MDA content. After salt stress for 15 days, roots, and leaves were harvested, rinsed with deionized water and wiped with tissues. Thereby, they were dried at 105°C for 10 min, and then dried at 70°C to constant weight for measuring $Na^+$ content.

### Measurements of Gas Exchange and Chlorophyll Fluorescence Parameters

Gas exchange and modulated chlorophyll fluorescence parameters were simultaneously detected by using an open photosynthetic system (LI-6400XTR, Li-Cor, Lincoln, NE,

USA) equipped with a fluorescence leaf chamber (6400-40 LCF, Li-Cor).

The leaves were dark-adapted for 30 min before the measurements. The minimal fluorescence level in the dark adapted state was measured using a modulated pulse ($< 0.05$ $\mu$mol m$^{-2}$ s$^{-1}$ for 1.8 s). Maximal fluorescence was measured after applying a saturating actinic light pulse of 8000 $\mu$mol m$^{-2}$ s$^{-1}$ for 0.7 s. Subsequently, actinic light intensity was altered to 1000 $\mu$mol m$^{-2}$ s$^{-1}$ in leaf cuvette and then maintained for about 30 min. The temperature, $CO_2$ concentration and relative humidity were, respectively, set at 25°C, 400 $\mu$mol mol$^{-1}$ and 65% in the leaf cuvette. Pn, $g_s$ and Ci were simultaneously recorded. In addition, steady-state fluorescence yield was also recorded. Then, a saturating actinic light pulse of 8000 $\mu$mol m$^{-2}$ s$^{-1}$ for 0.7 s was used to produce maximum fluorescence yield by temporarily inhibiting PSII photochemistry, and the minimum fluorescence in the steady state was determined during a brief interruption of actinic light irradiation in the presence of far-red light ($\lambda = 740$ nm). At last, ΦPSII and NPQ were calculated (Maxwell and Johnson, 2000).

For the measurement of CE, photon flux density and temperature were set at 1000 $\mu$mol m$^{-2}$ s$^{-1}$ and 25°C in the leaf cuvette. Pn was measured under $CO_2$ concentrations in a sequence of 700, 500, 400, 300, 200, 150, 100, and 50 $\mu$mol mol$^{-1}$. The leaves were kept under each level of $CO_2$ concentration for 4 min to let leaves reach steady-state photosynthesis, and Pn and Ci were then recorded. The correlation curve of Pn related to Ci was established, and CE was calculated from the linear portion of Pn-Ci curve.

### Measurement of Chlorophyll *a* Fluorescence and Modulated 820 nm Reflection Transients

The measurements were made by using a multifunctional plant efficiency analyzer (MPEA, Hansatech, UK), and the operating mechanism of this instrument has been elucidated in detail (Strasser et al., 2010; Kalaji et al., 2012). The leaves were adapted in dark for 30 min before the measurement (Kalaji et al., 2014b). Thereafter, the leaves were orderly illuminated with 1 s red light (627 nm, 5000 $\mu$mol photons m$^{-2}$ s$^{-1}$), 10 s far red light (735 nm, 200 $\mu$mol photons m$^{-2}$ s$^{-1}$) and 2 s red light (627 nm, 5000 $\mu$mol photons m$^{-2}$ s$^{-1}$). Chlorophyll *a* fluorescence and modulated 820 nm reflection were simultaneously recorded during the illumination. Monitoring modulated reflection change near 820 nm is a very convenient way to follow the redox state of PSI. The relative value of the maximal difference of 820 nm reflection during the last 2 s red illumination was used to indicate ΔMR/MR$_0$ (Schansker et al., 2003). MR$_0$ is the value of 820 nm reflection at 0.7 ms (the first reliable MR measurement). ΔMR is the value of the maximal difference of 820 nm reflection at the last 2 s red light illumination.

Chlorophyll *a* fluorescence transients were quantified according to JIP test by using the following original data: (1) fluorescence intensity at 20 $\mu$s (Fo, when all reaction centers of PSII are open); (2) the maximum fluorescence intensity (Fm, when all reaction centers of PSII are closed) and (3) fluorescence intensities at 300 $\mu$s (F$_k$, K step) and 2 ms (F$_J$, J step). Using these original data, some parameters can be calculated

for quantifying PSII behavior (Strasser et al., 2010). Fv/Fm, W$_k$ and ETo/ABS was, respectively, calculated as: Fv/Fm = (Fm − Fo)/Fm, W$_k$ = (F$_k$ − Fo)/(F$_J$ − Fo) and ETo/ABS = (Fm − F$_J$)/Fm.

### Measurements of Na$^+$ Content and Na$^+$ Translocation Factor

The extraction of Na$^+$ was performed according to Song et al. (2011). Deionized $H_2O$ (25 ml) was added to 0.1 g dried plant powder and boiled for 2 h. The supernatant was diluted 50 times with deionized $H_2O$ for measuring Na$^+$ content by using an atomic absorption spectrophotometer (TAS-990, China). Na$^+$ translocation factor was calculated as the ratio of Na$^+$ concentration between leaves and roots.

### Measurement of Root Na$^+$ Flux

Net Na$^+$ flux was measured using NMT (NMT system BIO-IM, Younger, USA). The concentration gradients of the target ions were measured by moving the ion-selective microelectrode between two positions close to the plant material in a pre-set excursion (20 $\mu$m for excised roots in the present experiment). The ion fluxes were calculated based on the Fick's law of diffusion.

Prepulled and silanized glass micropipettes (Xuyue Sci. and Tech., China) were firstly filled with a backfilling solution (100 mM NaCl) to a length of approximately 1 cm from the tip. Then the micropipettes were front filled with selective liquid ion-exchange cocktails (LIXs: Na, Sigma 71178). An Ag/AgCl wire electrode holder (Xuyue Sci. and Tech., China) was then inserted in the back of the electrode to make electrical contact with the electrolyte solution. DRIREF-2 (World Precision Instruments) was used as the reference electrode. Ion-selective electrodes were firstly calibrated before flux measurement using the following solutions: 5, 2, 0.5 mM Na$^+$. Only electrodes with Nernstian slopes $> 50$ mV/decade were used. Ion flux was calculated by Fick's law of diffusion: J = −D(dc/dx) where J represents the ion flux in the x direction, dc/dx is the ion concentration gradient, and D is the ion diffusion constant in a particular medium. Data and image acquisition, preliminary processing, control of the three-dimensional electrode positioner, and stepper-motor-controlled fine focus of the microscope stage were performed with IM-Flux software.

Newly developed root segments (5 cm from apex) were sampled, rinsed with deionized water and immediately incubated in the measuring solution to equilibrate for 30 min. Thereafter, roots were transferred to the measuring chamber containing 15 ml fresh measuring solution. Na$^+$ measuring solutions were as follows: 0.1 mM KCl, 0.1 mM CaCl$_2$, 0.1 mM MgCl$_2$, 2 mM NaCl, 0.3 mM MES, pH 6.0 (adjusted with choline and HCl). After the roots were immobilized on the bottom, ion flux measurements were started. Ion flux measurements were started from the apex and went along the root axis until 3000 $\mu$m at interval of 500 $\mu$m. The measured root positions could be visualized and defined under the NMT microscope (**Figure 1A**). As shown in **Figure 1B**, Na$^+$ efflux along the root axes was increased by salt stress, and according to these data, the average value of Na$^+$ efflux was calculated and shown in **Table 1**.
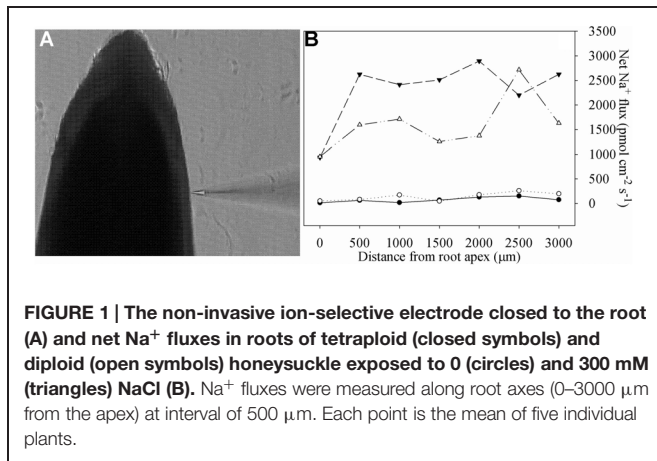
FIGURE 1 | The non-invasive ion-selective electrode closed to the root (A) and net $Na^+$ fluxes in roots of tetraploid (closed symbols) and diploid (open symbols) honeysuckle exposed to 0 (circles) and 300 mM (triangles) NaCl (B). $Na^+$ fluxes were measured along root axes (0–3000 μm from the apex) at interval of 500 μm. Each point is the mean of five individual plants.

## Measurement of MDA Content

Leaf tissues (0.5 g) were ground under liquid nitrogen and then homogenized in 5 ml of 50 mM potassium phosphate buffer (pH 7.8). After centrifugation at 4°C and 13000 × $g$ for 10 min, the supernatant was prepared for the assay of MDA content (Yan et al., 2010).

## Statistical Analysis

One-way ANOVA was carried out by using SPSS 16.0 (SPSS Inc., Chicago, IL, USA) for all sets of data. The values presented are the means of measurements with five replicate plants, and comparisons of means were determined through LSD test. Difference was considered significant at $P < 0.05$.

## Results

### Effects of Salt Stress on Biomass, $Na^+$ and MDA Content and Root $Na^+$ Flux

Leaf and root dry weight per plant were significantly decreased, respectively, by 24.24 and 33.67% in TH and by 54.17 and 53.49% in DH after salt stress, and the decrease was greater in DH (**Table 1**). Salt stress significantly increased leaf and root $Na^+$ content by 86.88 and 77.29% in TH, and the greater increase with 275.54 and 164.29% was found in DH. Root $Na^+$ efflux was elevated by 10.27 fold in DH after salt stress, and the greater

increase with 29.72 fold was found in TH. $Na^+$ translocation factor was significantly increased by 44.33% in DH after salt stress, but no significant change was noted in TH, suggesting that $Na^+$ transport to the leaf was restricted in TH. The extent of lipid peroxidation represented by MDA content reflects the state and integrity of membranes in plant cells (Blokhina et al., 2003; Yazici et al., 2007). Leaf MDA content was not significantly affected in TH after salt stress, whereas the significant increase was observed in DH.

### Effects of Salt Stress on Gas Exchange and Chlorophyll Fluorescence Parameters

Pn, $g_s$ and ΦPSII were significantly decreased in the leaves of TH and DH under salt stress, and the decrease was greater in DH than TH (**Figures 2A,B,E**). Under salt stress, Ci was lowered in the leaves of TH, but Ci in the leaves of DH was not significantly changed and even remarkably elevated at day 15 (**Figure 2C**). Under salt stress, CE in the leaves of DH was significantly decreased at day 3, whereas the significant decrease in CE was not recorded in the leaves of TH until day 11, and the decrease was lower than that in DH (**Figure 2D**). NPQ in the leaves of TH and DH was significantly increased by salt stress (**Figure 2F**).
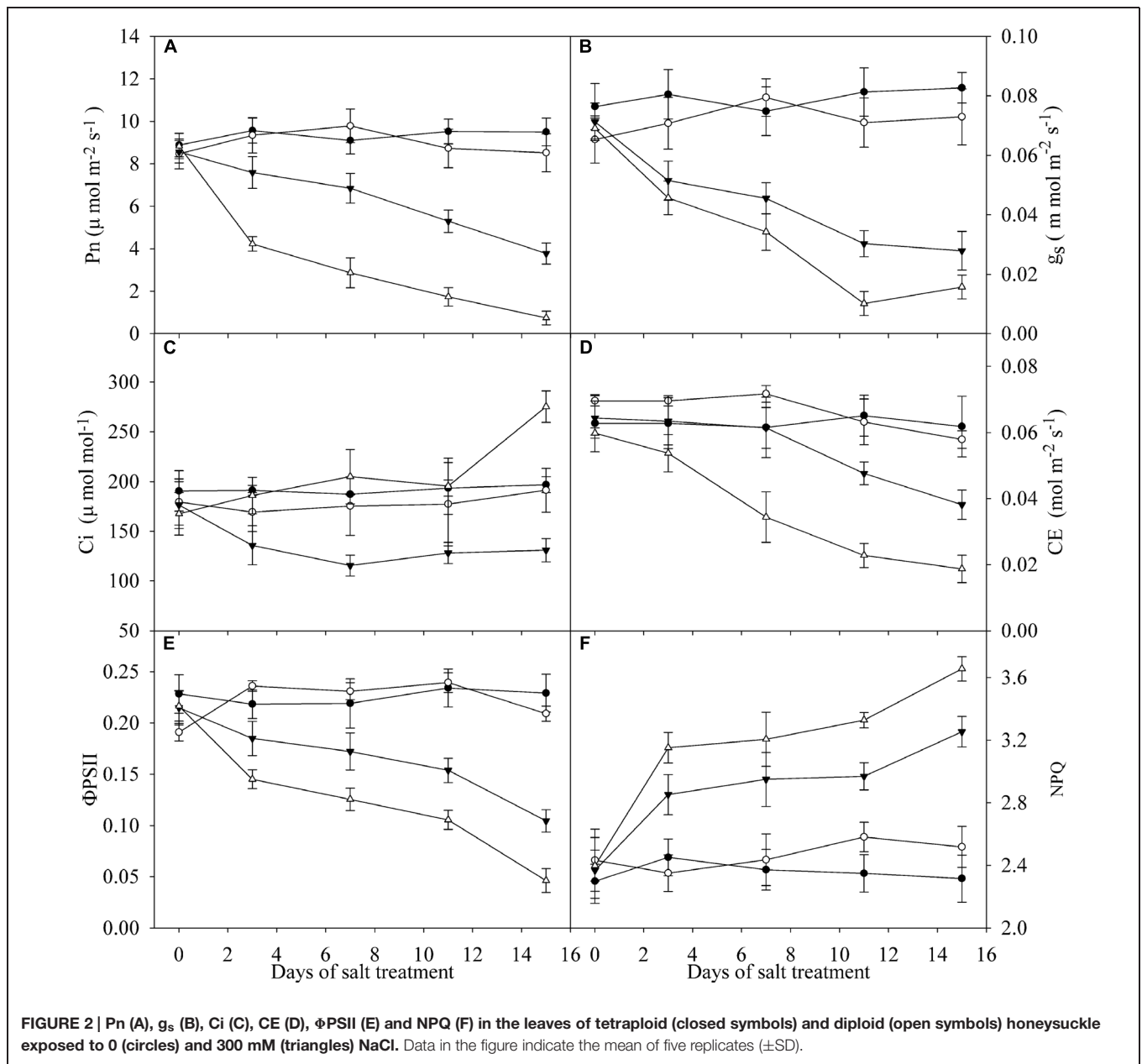
### Effects of Salt Stress on Chlorophyll *a* Fluorescence and Modulated 820 nm Reflection Transients

Salt stress did not obviously affect chlorophyll *a* fluorescence transients and 820 nm reflection transients in the leaves of TH (**Figures 3A,B**). Chlorophyll *a* fluorescence was declined under salt stress in the leaves of DH, indicating PSII capacity was negatively affected (**Figure 3C**). The 820 nm reflection signals are presented by $MR/MR_0$ ratio, where $MR_0$ is the value at the onset of actinic illumination (at 0.7 ms). Decrease in $MR/MR_0$ from $MR_0$ to the minimal value ($MR_{min}$, at about 29 ms) reflects PSI oxidation process, and the oxidation amplitude in the first 1 s red illumination was expressed as $MR_0 − MR_{min}$. The minimal value of MR is a transitory steady state with equal oxidation and re-reduction rate of PSI. Subsequently, increase in $MR/MR_0$ indicates PSI re-reduction driven by the electron flow from PSII. Thus, 820 nm reflection transient in the first 1 s red illumination was influenced by both PSII and PSI capacity and could reflect

TABLE 1 | Leaf and root dry weight per plant, leaf and root $Na^+$ content, $Na^+$ translocation factor and mean of root $Na^+$ flux in TH and DH exposed to 0 and 300 mM NaCl.

| Parameters | TH (0 mM) | TH (300 mM) | DH (0 mM) | DH (300 mM) |
|---|---|---|---|---|
| Leaf DW(g/plant) | 3.30 ± 0.24a | 2.50 ± 0.11b | 2.64 ± 0.17b | 1.21 ± 0.21c |
| Root DW(g/plant) | 0.98 ± 0.08a | 0.65 ± 0.04b | 0.86 ± 0.09ab | 0.40 ± 0.04c |
| Leaf $Na^+$ content(mg $g^{-1}$ DW) | 8.69 ± 0.88c | 16.24 ± 1.06b | 8.79 ± 0.76c | 33.01 ± 1.76a |
| Leaf MDA content(mg $g^{-1}$ DW) | 0.68 ± 0.06b | 0.69 ± 0.05b | 0.70 ± 0.03b | 1.17 ± 0.07a |
| Root $Na^+$ content(mg $g^{-1}$ DW) | 14.75 ± 3.02c | 26.15 ± 3.04b | 13.16 ± 0.93c | 34.78 ± 2.68a |
| $Na^+$ translocation factor | 1.91 ± 0.25b | 2.28 ± 0.19b | 2.03 ± 0.32b | 2.93 ± 0.25a |
| Mean of root $Na^+$ efflux (pmol $cm^{-2}$ $s^{-1}$) | 75.36 ± 10.37c | 2315.27 ± 242.62a | 185.32 ± 56.23c | 1605.03 ± 289.27b |

*DW indicates dry weight. Data in the table indicate the mean of five replicates (±SD). Within each row, means followed by the same letters are not significantly different at P < 0.05.*

**FIGURE 2 | Pn (A), $g_s$ (B), Ci (C), CE (D), ΦPSII (E) and NPQ (F) in the leaves of tetraploid (closed symbols) and diploid (open symbols) honeysuckle exposed to 0 (circles) and 300 mM (triangles) NaCl.** Data in the figure indicate the mean of five replicates (±SD).

their coordination. The 820 nm reflection transient was obviously changed in the leaves of DH under salt stress, indicating the negative effects on PSII and PSI coordination. PSI oxidation amplitude was significantly decreased in the leaves of DH under salt stress, whereas no significant change occurred in the leaves of TH (The inserted panels of **Figures 3B,D**).
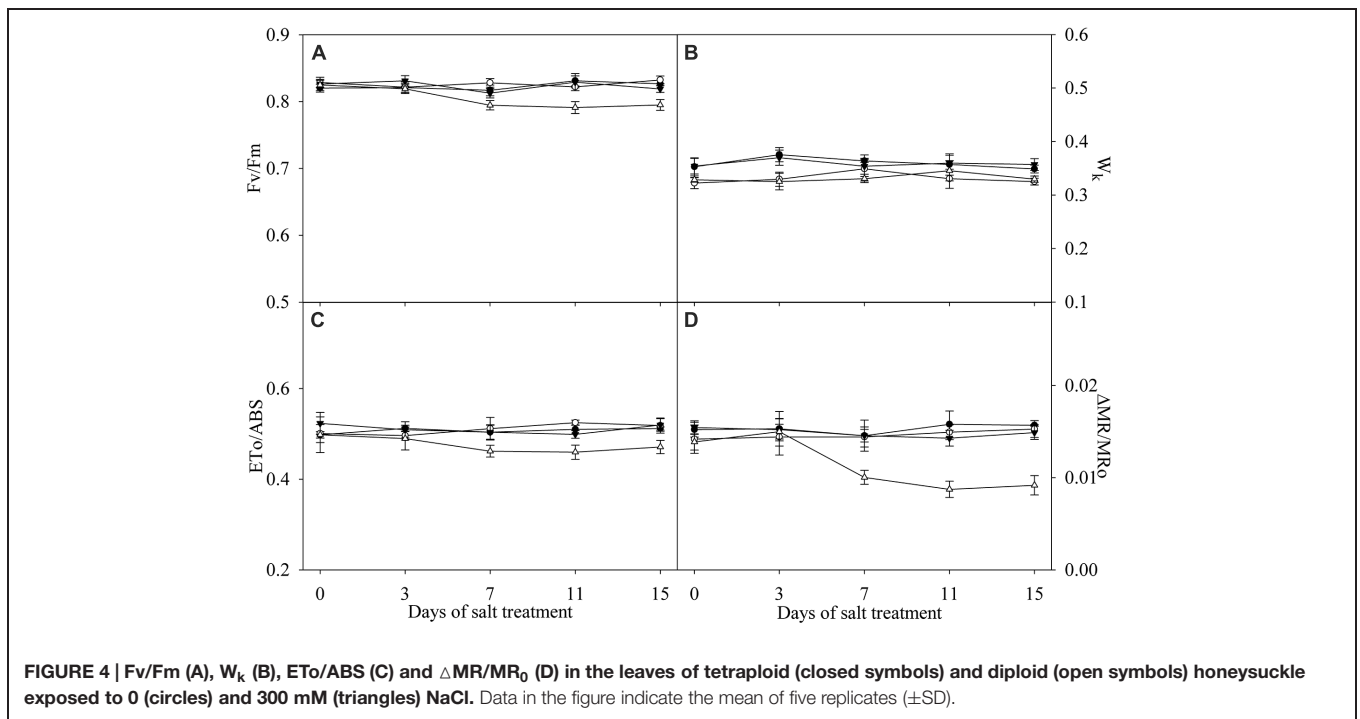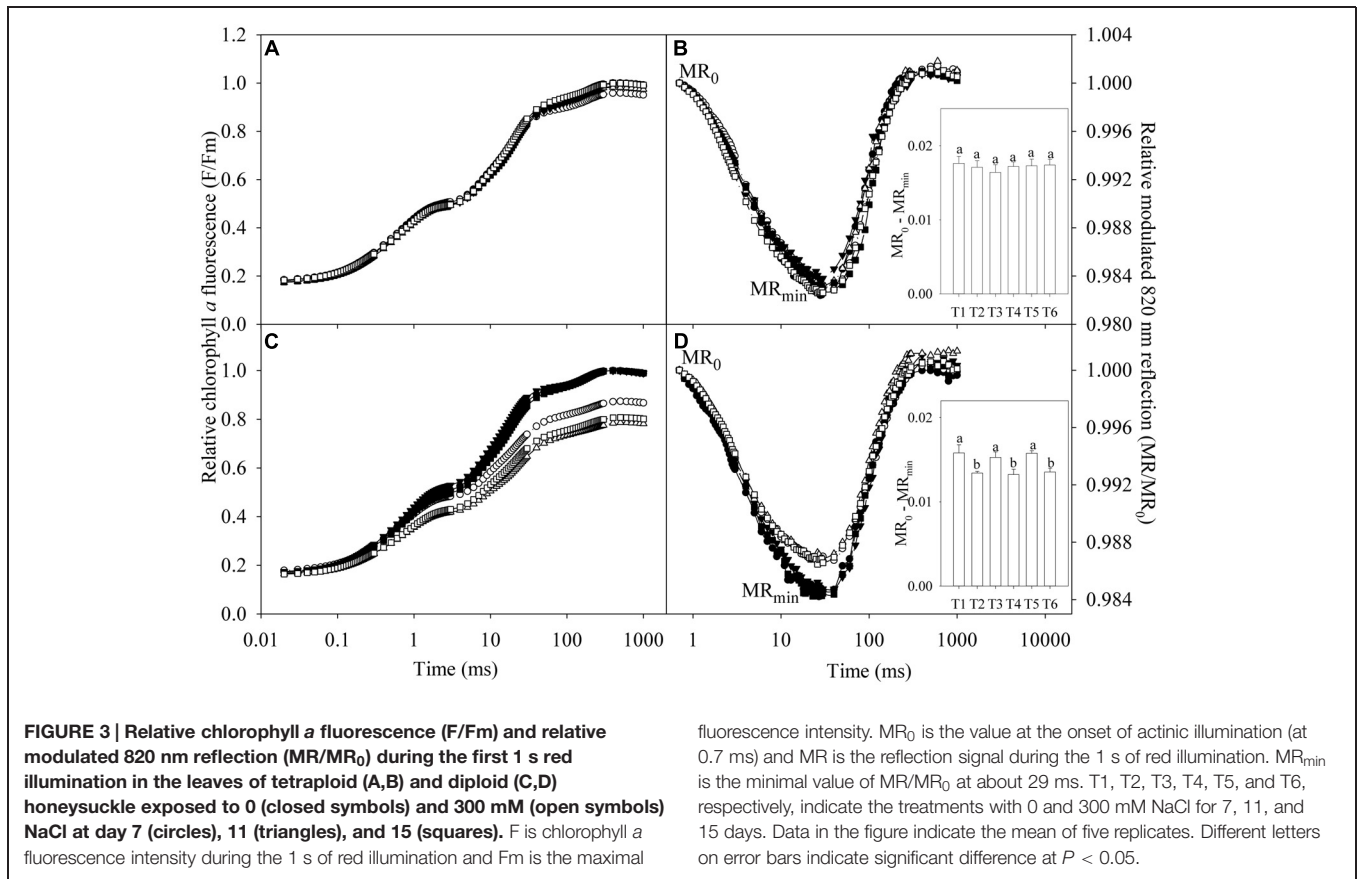
### Effects of Salt Stress on Fv/Fm, $W_k$, ETo/ABS, and ΔMR/$MR_0$

Under salt stress, Fv/Fm, $W_k$, ETo/ABS, and ΔMR/$MR_0$ were not significantly affected in the leaves of TH (**Figure 4**). Significant decrease in Fv/Fm, ETo/ABS, and ΔMR/$MR_0$ was found in the leaves of DH after 7 days of salt stress (**Figures 4A,C,D**), indicating the occurrence of PSII and PSI photoinhibition.

Increase in $W_k$ with an elevated K step around 300 μs in chlorophyll *a* fluorescence transient is a specific indicator of injury on OEC (Strasser, 1997; Kalaji et al., 2014a). Insignificant change in $W_k$ and no obvious K step indicated that OEC was not damaged in the leaves of DH and TH under salt stress (**Figures 3A,C** and **4B**).

## Discussion

Plant photosynthesis and growth are commonly constrained in saline environment, and salt-tolerant plants can better adapt to salinity with less decrease in biomass and photosynthetic capacity (Kalaji and Nalborczyk, 1991; Stepien and Johnson, 2009;

**FIGURE 3 | Relative chlorophyll *a* fluorescence (F/Fm) and relative modulated 820 nm reflection (MR/MR$_0$) during the first 1 s red illumination in the leaves of tetraploid (A,B) and diploid (C,D) honeysuckle exposed to 0 (closed symbols) and 300 mM (open symbols) NaCl at day 7 (circles), 11 (triangles), and 15 (squares).** F is chlorophyll *a* fluorescence intensity during the 1 s of red illumination and Fm is the maximal fluorescence intensity. MR$_0$ is the value at the onset of actinic illumination (at 0.7 ms) and MR is the reflection signal during the 1 s of red illumination. MR$_{min}$ is the minimal value of MR/MR$_0$ at about 29 ms. T1, T2, T3, T4, T5, and T6, respectively, indicate the treatments with 0 and 300 mM NaCl for 7, 11, and 15 days. Data in the figure indicate the mean of five replicates. Different letters on error bars indicate significant difference at $P < 0.05$.



**FIGURE 4 | Fv/Fm (A), W$_k$ (B), ETo/ABS (C) and △MR/MR$_0$ (D) in the leaves of tetraploid (closed symbols) and diploid (open symbols) honeysuckle exposed to 0 (circles) and 300 mM (triangles) NaCl.** Data in the figure indicate the mean of five replicates (±SD).

Chao et al., 2013; Aparicio et al., 2014). In this study, stronger salt tolerance was defined in TH, because TH maintained higher photosynthetic capacity and accumulated greater biomass than DH under salt stress (**Table 1**; **Figure 2**).

Photosynthetic rate, $g_s$ and Ci in TH concomitantly declined under salt stress, suggesting the stomatal limitation on photosynthesis (**Figures 2A–C**; Farquhar and Sharkey, 1982). The declined $g_s$ can serve as a protective way against salt-induced osmotic stress by reducing water loss from transpiration, but increases the stomatal limitation of photosynthesis (Chaves et al., 2009). TH has stronger osmotic adjusting ability than DH due to the morphological and anatomical characterizations (Li et al., 2009), and therefore, TH maintained higher leaf $g_s$ under salt stress, which helped to alleviate stomatal limitation on photosynthesis. The salt-induced change in Ci was not coincident with Pn and $g_s$ in DH (**Figures 2A–C**), suggesting that stomatal limitation did not play a major role in the decrease of Pn. CE positively correlates with Rubisco activity (Voncaemmerer and Farquhar, 1981). The declined CE indicated $CO_2$ fixation was depressed, and the greater inhibition on $CO_2$ fixation in DH possibly resulted in more severe oxidative stress on photosystem (**Figure 2D**). Allakhverdiev et al. (2002) reported that salt stress induced PSII photoinhibition in *Synechocystis* by inhibiting the repair of photodamaged PSII not by directly accelerating photodamage on OEC. In this study, PSII photoinhibition without injury on OEC in DH also implied the negative effects of salt stress on PSII repair (**Figures 4A,B**). As the traditional viewpoint, PSII is more susceptible to abiotic stresses than PSI, and PSII photoinhibition can protect PSI against photoinhibition by reducing the electron transport to PSI, however, PSI photoinhibition is more liable to occur just under chilling stress with low light due to the less inhibition on electron flow from PSII (Scheller and Haldrup, 2005). PSII photoinhibition reduced the electron flow to PSI in DH (**Figure 4C**), and consistently, the declined ΦPSII suggested that the actual photosynthetic electron transport from PSII was lowered after photosynthesis starting (**Figure 2E**). However, the inhibition on electron flow was not enough to protect PSI from photoinhibition (**Figure 4D**). Due to PSI photoinhibition, electrons could not be effectively driven to the acceptor side of PSI, and PSI oxidation would be shortened in the first 1 s red illumination. On the contrary, the declined electron flow from PSII could delay PSI re-reduction and prolong PSI oxidation. On the basis of the significant decrease in PSI oxidative amplitude (Inserted panels in **Figures 3B,D**), we can deduce that PSI photoinhibition was more severe than PSII photoinhibition in DH upon salt stress. As a result, the coordination between PSI and PSII was destroyed. In contrast, PSI and PSII photoinhibition in TH did not occur under salt stress in spite of the remarkable decrease in $CO_2$ fixation (**Figure 4D**), because the increased NPQ helped to dissipate

the excess excitation energy and potentially limit ROS production (**Figure 2F**). In consequence, the normal coordination between PSI and PSII was maintained in TH under salt stress. Similarly, normal PSI and PSII capacity was maintained in the halophyte *Thellungiella* under salt stress at 500 mM NaCl, but the effects on photosynthetic $CO_2$ fixation and NPQ were not significant, indicating that its photosystem might not be endangered by the excess excitation energy (Stepien and Johnson, 2009). In agreement with the occurrence of photoinhibition, the extent of leaf lipid peroxidation in DH was significantly elevated by salt stress (**Table 1**), confirming the oxidative damage of ROS. Comparatively, no significant change was observed in leaf lipid peroxidation in TH after salt stress (**Table 1**), and this result was in accordance with the insignificant oxidative effects on photosystem.

$Na^+$ is the primary toxic component for plants upon salt stress (Munns and Tester, 2008). $Na^+$ can inhibit $CO_2$ fixation by inducing negative effects on Rubisco, lead to the increase of ROS generation and irreversibly inactivate PSII and PSI (Allakhverdiev et al., 2000; Murata et al., 2007; Oukarroum et al., 2015). Thus, salt sensitive plant varieties tend to accumulate more $Na^+$ in the leaf under salt stress and exhibit severe toxic symptoms (Chen et al., 2013; Aparicio et al., 2014). As an underlying reason for the higher salt tolerance, TH accumulated less $Na^+$ in the leaf in contrast to DH under salt stress (**Table 1**). Consistently, salt-induced decrease in $CO_2$ fixation was lower in the leaves of TH (**Figure 2D**), and as a result, PSII and PSI photoinhibition was not induced in line with no significant changes in lipid peroxidation (**Table 1**; **Figure 4**). It has been proposed that the divergence between salt tolerant and salt sensitive plants originates in the control of uptake and internal $Na^+$ transport (Bojorquez-Quintal et al., 2014; Maathuis et al., 2014). Accordingly, we revealed that the lower leaf $Na^+$ concentration in TH depended on the greater elevation of root $Na^+$ extrusion and restriction of $Na^+$ transport from root to leaf (**Table 1**).

## Conclusion

TH maintained normal PSII and PSI coordination by preventing photoinhibition and exhibited higher leaf photosynthetic activity than DH under salt stress. The higher leaf photosynthetic activity which contributed to biomass accumulation in TH might be ascribed to the lower ionic toxicity of $Na^+$.

## Acknowledgment

## References

Allakhverdiev, S. I., Nishiyama, Y., Miyairi, S., Yamamoto, H., Inagaki, N., Kanesaki, Y., et al. (2002). Salt stress inhibits the repair of photodamaged photosystem II by suppressing the transcription and translation of psbA genes in *Synechocystis*. *Plant Physiol.* 130, 1443–1453. doi: 10.1104/pp. 011114

Allakhverdiev, S. I., Sakamoto, A., Nishiyama, Y., Inaba, M., and Murata, N. (2000). Ionic and osmotic effects of NaCl-induced inactivation of photosystems I and II in *Synechococcus* sp. *Plant Physiol.* 123, 1047–1056. doi: 10.1104/pp.123. 3.1047

Aparicio, C., Urrestarazu, M., and Cordovilla, M. D. (2014). Comparative physiological analysis of salinity effects in six olive genotypes. *HortScience* 49, 901–904.

Bilger, W., and Bjorkman, O. (1990). Role of the xanthophyll cycle in photoprotection elucidated by measurements of light-induced absorbance changes, fluorescence and photosynthesis in leaves of *Hedera Canariensis*. *Photosynth. Res.* 25, 173–185. doi: 10.1007/BF00033159

Blokhina, O., Virolainen, E., and Fagerstedt, K. V. (2003). Antioxidants, oxidative damage and oxygen deprivation stress: a review. *Ann. Bot.* 91, 179–194. doi: 10.1093/Aob/Mcf118

Bojorquez-Quintal, E., Velarde-Buendia, A., Ku-Gonzalez, A., Carillo-Pech, M., Ortega-Camacho, D., EchevarrIa-Machado, I., et al. (2014). Mechanisms of salt tolerance in habanero pepper plants (*Capsicum chinense* Jacq.): proline accumulation, ions dynamics and sodium root-shoot partition and compartmentation. *Front. Plant Sci.* 5:605. doi: 10.3389/fpls.2014.00605

Brestic, M., Zivcak, M., Olsovska, K., Shao, H. B., Kalaji, H. M., and Allakhverdiev, S. I. (2014). Reduced glutamine synthetase activity plays a role in control of photosynthetic responses to high light in barley leaves. *Plant Physiol. Biochem.* 81, 74–83. doi: 10.1016/j.plaphy.2014.01.002

Carbonera, D., Gerotto, C., Posocco, B., Giacometti, G. M., and Morosinotto, T. (2012). NPQ activation reduces chlorophyll triplet state formation in the moss *Physcomitrella patens*. *Biochim. Biophys. Acta* 1817, 1608–1615. doi: 10.1016/j.bbabio.2012.05.007

Chao, D. Y., Dilkes, B., Luo, H. B., Douglas, A., Yakubova, E., Lahner, B., et al. (2013). Polyploids exhibit higher potassium uptake and salinity tolerance in *Arabidopsis*. *Science* 341, 658–659. doi: 10.1126/science.1240561

Chaves, M. M., Flexas, J., and Pinheiro, C. (2009). Photosynthesis under drought and salt stress: regulation mechanisms from whole plant to cell. *Ann. Bot.* 103, 551–560. doi: 10.1093/Aob/Mcn125

Chen, H. X., Li, W. J., An, S. Z., and Gao, H. Y. (2004). Characterization of PSII photochemistry and thermostability in salt-treated *Rumex* leaves. *J. Plant Physiol.* 161, 257–264. doi: 10.1078/0176-1617-01231

Chen, P., Yan, K., Shao, H., and Zhao, S. (2013). Physiological mechanisms for high salt tolerance in wild soybean (*Glycine soja*) from yellow river delta, China: photosynthesis, osmotic regulation, ion flux and antioxidant capacity. *PLoS ONE* 8:e83227. doi: 10.1371/journal.pone.0083227

Farquhar, G. D., and Sharkey, T. D. (1982). Stomatal conductance and photosynthesis. *Ann. Rev. Plant Physiol.* 33, 317–345. doi: 10.1146/annurev.pp.33.060182.001533

Feng, L. L., Han, Y. J., Liu, G., An, B. G., Yang, J., Yang, G. H., et al. (2007). Overexpression of sedoheptulose-1,7-bisphosphatase enhances photosynthesis and growth under salt stress in transgenic rice plants. *Funct. Plant Biol.* 34, 822–834. doi: 10.1071/Fp07074

Herrmann, B., Kilian, R., Peter, S., and Schafer, C. (1997). Light-stress-related changes in the properties of photosystem I. *Planta* 201, 456–462. doi: 10.1007/s004250050089

Hussain, S., Luro, F., Costantino, G., Ollitrault, P., and Morillon, R. (2012). Physiological analysis of salt stress behaviour of citrus species and genera: low chloride accumulation as an indicator of salt tolerance. *S. Afr. J. Bot.* 81, 103–112. doi: 10.1016/j.sajb.2012.06.004

Kalaji, H. M., Goltsev, V., Bosa, K., Allakhverdiev, S. I., Strasser, R. J., and Govindjee (2012). Experimental in vivo measurements of light emission in plants: a perspective dedicated to David Walker. *Photosynth. Res.* 114, 69–96. doi: 10.1007/s11120-012-9780-3

Kalaji, H. M., Govindjee, Bosa, K., Koscielniak, J., and Zuk-Golaszewska, K. (2011). Effects of salt stress on photosystem II efficiency and $CO_2$ assimilation of two Syrian barley landraces. *Environ. Exp. Bot.* 73, 64–72. doi: 10.1016/j.envexpbot.2010.10.009

Kalaji, H. M., and Nalborczyk, E. (1991). Gas exchange of barley seedlings growing under salinity stress. *Photosynthetica* 25, 197–202.

Kalaji, H. M., Oukarroum, A., Alexandrov, V., Kouzmanova, M., Brestic, M., Zivcak, M., et al. (2014a). Identification of nutrient deficiency in maize and tomato plants by in vivo chlorophyll a fluorescence measurements. *Plant Physiol. Biochem.* 81, 16–25. doi: 10.1016/j.plaphy.2014.03.029

Kalaji, H. M., Schansker, G., Ladle, R. J., Goltsev, V., Bosa, K., Allakhverdiev, S. I., et al. (2014b). Frequently asked questions about in vivo chlorophyll fluorescence: practical issues. *Photosynth. Res.* 122, 121–158. doi: 10.1007/s11120-014-0024-6

Kalaji, H. M., and Pietkiewicz, S. (1993). Salinity effects on plant growth and other physiological processes. *Acta Physiol. Plant.* 15, 89–124.

Kudoh, H., and Sonoike, K. (2002). Irreversible damage to photosystem I by chilling in the light: cause of the degradation of chlorophyll after returning to normal growth temperature. *Planta* 215, 541–548. doi: 10.1007/s00425-002-0790-9

Li, W. D., Biswas, D. K., Xu, H., Xu, C. Q., Wang, X. Z., Liu, J. K., et al. (2009). Photosynthetic responses to chromosome doubling in relation to leaf anatomy in *Lonicera japonica* subjected to water stress. *Funct. Plant Biol.* 36, 783–792. doi: 10.1071/Fp09022

Loreto, F., Centritto, M., and Chartzoulakis, K. (2003). Photosynthetic limitations in olive cultivars with different sensitivity to salt stress. *Plant Cell Environ.* 26, 595–601. doi: 10.1046/j.1365-3040.2003.00994.x

Lu, K. X., Cao, B. H., Feng, X. P., He, Y., and Jiang, D. A. (2009). Photosynthetic response of salt-tolerant and sensitive soybean varieties. *Photosynthetica* 47, 381–387. doi: 10.1007/s11099-009-0059-7

Maathuis, F. J. M., Ahmad, I., and Patishtan, J. (2014). Regulation of $Na^+$ fluxes in plants. *Front. Plant Sci.* 5:467. doi: 10.3389/fpls.2014.00467

Maxwell, K., and Johnson, G. N. (2000). Chlorophyll fluorescence – a practical guide. *J. Exp. Bot.* 51, 659–668. doi: 10.1093/jexbot/51.345.659

Meng, H. B., Jiang, S. S., Hua, S. J., Lin, X. Y., Li, Y. L., Guo, W. L., et al. (2011). Comparison between a tetraploid turnip and its diploid progenitor (*Brassica rapa* L.): the adaptation to salinity stress. *Agric. Sci. China* 10, 363–375. doi: 10.1016/S1671-2927(11)60015-1

Mouhaya, W., Allario, T., Brumos, J., Andres, F., Froelicher, Y., Luro, F., et al. (2010). Sensitivity to high salinity in tetraploid citrus seedlings increases with water availability and correlates with expression of candidate genes. *Funct. Plant Biol.* 37, 674–685. doi: 10.1071/FP10035

Muller, P., Li, X. P., and Niyogi, K. K. (2001). Non-photochemical quenching. A response to excess light energy. *Plant Physiol.* 125, 1558–1566. doi: 10.1104/pp.125.4.1558

Munns, R., and Tester, M. (2008). Mechanisms of salinity tolerance. *Annu. Rev. Plant Biol.* 59, 651–681. doi: 10.1146/annurev.arplant.59.032607.092911

Murata, N., Takahashi, S., Nishiyama, Y., and Allakhverdiev, S. I. (2007). Photoinhibition of photosystem II under environmental stress. *Biochim. Biophys. Acta* 1767, 414–421. doi: 10.1016/j.bbabio.2006.11.019

Netondo, G. W., Onyango, J. C., and Beck, E. (2004). Sorghum and salinity: II. Gas exchange and chlorophyll fluorescence of sorghum under salt stress. *Crop Sci.* 44, 806–811. doi: 10.2135/cropsci2004.0806

Oukarroum, A., Bussotti, F., Goltsev, V., and Kalaji, H. M. (2015). Correlation between reactive oxygen species production and photochemistry of photosystems I and II in *Lemna gibba* L. plants under salt stress. *Environ. Exp. Bot.* 109, 80–88. doi: 10.1016/j.envexpbot.2014.08.005

Schansker, G., Srivastava, A., Govindjee., and Strasser, R. J. (2003). Characterization of the 820-nm transmission signal paralleling the chlorophyll a fluorescence transient (OJIP) in pea leaves. *Funct. Plant Biol.* 30, 785–796. doi: 10.1071/FP03032

Scheller, H. V., and Haldrup, A. (2005). Photoinhibition of photosystem I. *Planta* 221, 5–8. doi: 10.1007/s00425-005-1507-7

Song, J., Shi, G. W., Gao, B., Fan, H., and Wang, B. S. (2011). Waterlogging and salinity effects on two *Suaeda salsa* populations. *Physiol. Plant.* 141, 343–351. doi: 10.1111/j.1399-3054.2011.01445.x

Sonoike, K. (1996). Degradation of psaB gene product, the reaction center subunit of photosystem I, is caused during photoinhibition of photosystem I: possible involvement of active oxygen species. *Plant Sci.* 115, 157–164. doi: 10.1016/0168-9452(96)04341-5

Sonoike, K. (2011). Photoinhibition of photosystem I. *Physiol. Plant.* 142, 56–64. doi: 10.1111/j.1399-3054.2010.01437.x

Stepien, P., and Johnson, G. N. (2009). Contrasting responses of photosynthesis to salt stress in the glycophyte *Arabidopsis* and the halophyte *Thellungiella*: role of the plastid terminal oxidase as an alternative electron sink. *Plant Physiol.* 149, 1154–1165. doi: 10.1104/pp.108.132407

Strasser, B. J. (1997). Donor side capacity of photosystem II probed by chlorophyll a fluorescence transients. *Photosynth. Res.* 52, 147–155. doi: 10.1023/A:1005896029778

Strasser, R. J., Tsimilli-Michael, M., Qiang, S., and Goltsev, V. (2010). Simultaneous in vivo recording of prompt and delayed fluorescence and 820 nm reflection changes during drying and after rehydration of the resurrection plant *Haberlea rhodopensis*. *Biochim. Biophys. Acta* 1797, 1313–1326. doi: 10.1016/j.bbabio.2010.03.008

Takahashi, S., and Murata, N. (2008). How do environmental stresses accelerate photoinhibition? *Trends Plant Sci.* 13, 178–182. doi: 10.1016/j.tplants.2008.01.005

Voncaemmerer, S., and Farquhar, G. D. (1981). Some relationships between the biochemistry of photosynthesis and the gas exchange of leaves. *Planta* 153, 376–387. doi: 10.1007/BF00384257

Wang, Z. M., Wang, M. Y., Liu, L., and Meng, F. J. (2013). Physiological and proteomic responses of diploid and tetraploid black locust (*Robinia pseudoacacia* L.) subjected to salt stress. *Int. J. Mol. Sci.* 14, 20299–20325. doi: 10.3390/ijms141020299

Yan, K., Chen, P., Shao, H. B., Shao, C. Y., Zhao, S. J., and Brestic, M. (2013a). Dissection of photosynthetic electron transport process in sweet sorghum under heat stress. *PLoS ONE* 8:e62100. doi: 10.1371/journal.pone.0062100

Yan, K., Chen, P., Shao, H. B., and Zhao, S. J. (2013b). Characterization of photosynthetic electron transport chain in bioenergy crop Jerusalem artichoke (*Helianthus tuberosus* L.) under heat stress for sustainable cultivation. *Ind. Crops Prod.* 50, 809–815. doi: 10.1016/j.indcrop.2013.08.012

Yan, K., Chen, W., He, X. Y., Zhang, G. Y., Xu, S., and Wang, L. L. (2010). Responses of photosynthesis, lipid peroxidation and antioxidant system in leaves of *Quercus mongolica* to elevated $O_3$. *Environ. Exp. Bot.* 69, 198–204. doi: 10.1016/j.envexpbot.2010.03.008

Yazici, I., Tuerkan, I., Sekmen, A. H., and Demiral, T. (2007). Salinity tolerance of purslane (*Portulaca oleracea* L.) is achieved by enhanced antioxidative system, lower level of lipid peroxidation and proline accumulation. *Environ. Exp. Bot.* 61, 49–57. doi: 10.1016/j.envexpbot.2007.02.010

Zhang, S. P., and Scheller, H. V. (2004). Photoinhibition of photosystem I at chilling temperature and subsequent recovery in *Arabidopsis thaliana*. *Plant Cell Physiol.* 45, 1595–1602. doi: 10.1093/pcp/pch180

Zhang, Z. S., Jia, Y. J., Gao, H. Y., Zhang, L. T., Li, H. D., and Meng, Q. W. (2011). Characterization of PSI recovery after chilling-induced photoinhibition in cucumber (*Cucumis sativus* L.) leaves. *Planta* 234, 883–889. doi: 10.1007/s00425-011-1447-3

Zivcak, M., Brestic, M., Kalaji, M. H., and Govindjee. (2014). Photosynthetic responses of sun- and shade-grown barley leaves to high light: is the lower PSII connectivity in shade leaves associated with protection against excess of light? *Photosynth. Res.* 119, 339–354. doi: 10.1007/s11120-014-9969-8